Effect of Polymer Degradation on Polymer Flooding in Homogeneous Reservoirs

Xiankang Xin[1], Gaoming Yu[2] , Ruicheng Ma[1], Keliu Wu[3] and Zhangxin Chen[1,3]

[1]*College of Petroleum Engineering, China University of Petroleum, Beijing, 102249 Beijing, China*
[2]*College of Petroleum Engineering, Yangtze University, 430100 Wuhan, China*
[3]*Department of Chemical and Petroleum Engineering, University of Calgary, T2N 1N4 Calgary, Canada*

Abstract. In this paper, physical and numerical simulations were applied to investigate the polymer degradation performance and its effect on polymer enhanced oil recovery (EOR) efficiency in homogeneous reservoirs. Physical experiments were conducted to determine basic physicochemical properties of the polymer, including viscosity, rheology, and degradation. A new mathematical model was proposed, and an in-house simulator was designed to further explore polymer degradation. The results of the physical experiments illustrated that polymer could increase polymer solution viscosity significantly, and the relationship between polymer solution viscosity and polymer concentration exhibited a clear power law relationship. However, the viscosity of a polymer solution with the same polymer concentration decreased with an increase in the shear rate, showing shear thinning performance. Moreover, the viscosity decreased with an increase in time, which was caused by polymer degradation. The validation of the designed simulator was improved when compared to the simulation results using ECLIPSE V2013.1 software. The difference between 0 and 0.1 day^{-1} in the polymer degradation rate showed a decrease of 6% in oil recovery after 2,000 days, according to simulation results, which demonstrated that polymer degradation had an adverse effect on polymer flooding efficiency.

1 Introduction

Polymers are closely related to our daily life. They have been widely applied in medicine, aerospace, the chemical industry and other fields [1–3]. Polymers have played a significant role, especially in the chemical industry. Polymer flooding, a mature chemical enhanced oil recovery (EOR) technology, has been used in oil field projects since the 1950s, where the viscosity of water was increased by adding polymer, and the water-oil mobility ratio was reduced [4]. The successful application of polymer flooding in oil and gas fields can alleviate the pressure from crude oil demand to a certain extent [5]. Therefore, polymer flooding is attracting increasing attention.

To make the best efficiency of polymer flooding, many researchers have done detailed research on the physicochemical properties of polymer; their studies mainly focused on the following aspects:

-Viscosity increasing. Many factors affect the viscosity of a polymer solution, such as temperature, polymer concentration, and the salinity of the water used in the solution preparation [6, 7].

-Rheological properties. A polymer solution often exhibits shear thinning within a certain range of shear rates [8, 9].

-Inaccessible pore volumes. An inaccessible pore volume is mainly influenced by permeability [10] and it affects the polymer flow in porous media [11].

-Absorption. Polymer adsorption depends on temperature, concentration, etc. [12].

-Degradation. Temperature, oxygen content and other factors affect polymer degradation [13, 14].

Polymer flooding simulation has also been carried out. With the continuous improvement of simulation research, most of the physicochemical properties of the polymer can be described in the simulation, but how to describe polymer degradation in a simulation has not been entirely solved. Some methods were used to solve this problem, but they did not work well. For example, because the application of the first order degradation model is based on concentration, it could not keep polymer concentration during polymer degradation [15].

In this paper, an experimental study was conducted to investigate some fundamental physicochemical properties of polymer including increasing viscosity, rheology, and degradation. A new mathematical model was proposed, and a novel in-house three-dimensional (3D) two-phase polymer flooding simulator was designed, with polymer degradation studies planned as part of the work scope. The validation of this simulator was done by comparing with the simulation results run in the ECLIPSE V2013.1 software. The simulations considering polymer degradation were undertaken using the designed

simulator to investigate the influence of the polymer degradation on production indicators including a pressure difference and oil production. These results and simulations offer a tool to study the effects of polymer degradation on polymer flooding in homogeneous reservoirs.

2 Methodology

2.1 Physical experiments

2.1.1 Rheology test

The properties of polymer and the ion components and their concentrations in the brine are shown in Table 1 and Table 2. After preparation of the polymer solution including pre-shearing, the rheological experiment was conducted on the Physica MCR301 advanced rotary rheometer from Anton Paar. The viscosity of the polymer solution with different concentrations was tested at the shear rate of 6.7 s^{-1}, and the viscosity of the polymer solution with a concentration of 1,500 mg/L was measured at different shear rates at 45 ^{o}C.

Table 1. The properties of the polymer.

Properties	Description/Value
Type	Partially hydrolyzed polyacrylamide (HPAM)
Molecular weight	2.2×10^7
Solid content, wt.%	90
Hydrolysis degree, %	25
Filtration factor	1.6
Dissolution rate, hour	<2
Insoluble matter, wt.%	0.2
Granularity ≥1.0 mm, %	5
Granularity ≤0.2 mm, %	2.5

Table 2. Ion components and their concentrations in the brine.

Ion components	Concentration, mg/L
Na^+ and K^+	173.38
Ca^{2+}	46.92
Mg^{2+}	29.97
HCO_3^-	526.35
SO_4^{2-}	5.92
Cl^-	127.46
TDS	910.00

2.1.2 Polymer degradation experiment

After being deoxidized, the prepared polymer solution with a concentration of 1,500 mg/L was sealed and placed in a thermotank at a temperature of 45 ^{o}C. The viscosity of polymer solutions was measured at 45 ^{o}C at 1 day, 5 day, 15 day, 20 day, 40 day, 60 day, 80 day,100 day and 120 day.

2.2 Mathematical model

The underlying assumptions are as follows.
- The flow was isothermal and followed Darcy's law.
- The model was 3D with two phases (oil and water).
- The rock was compressible and anisotropic, and the fluid was compressible.
- Polymer components only included high and low molecular weight polymer components. The viscosity of the polymer solution was determined by the high molecular weight polymer component.
- The virgin polymer solution polymer contained only the high molecular weight polymer component.
- The mixture of water and polymer is ideal, and they existed only in the water phase.
- The effects of the capillary force and gravity were taken into account.

According to the conservation of mass, the mass conservation equations of all components were obtained as follows.

For oil:

$$\nabla\cdot\left[\frac{\vec{k}k_{ro}}{\mu_o B_o}\left(\nabla p_o-\rho_o g\nabla D\right)\right]+q_o=\frac{\partial}{\partial t}\left(\frac{\phi s_o}{B_o}\right) \tag{1}$$

For water:

$$\nabla\cdot\left[\frac{\vec{k}k_{rw}}{\mu_{we} B_w R_k}\left(\nabla p_w-\rho_w g\nabla D\right)\right]+q_w=\frac{\partial}{\partial t}\left(\frac{\phi s_w}{B_w}\right) \tag{2}$$

For high molecular weight polymer component:

$$\nabla\cdot\left[\frac{\vec{k}k_{rw}c_{hp}}{\mu_{we} B_w R_k}\left(\nabla p_w-\rho_w g\nabla D\right)\right]-c_{hp}R_{pd}+q_w c_{hp}=\frac{\partial}{\partial t}\left(\frac{\phi(1-f_{ip})s_w c_{hp}}{B_w}\right)+\frac{\partial\left[(1-f_{ip})(1-\phi)\rho_r c_{hpa}\right]}{\partial t} \tag{3}$$

For low molecular weight polymer component:

$$\nabla\cdot\left[\frac{\vec{k}k_{rw}c_{lp}}{\mu_{we} B_w R_k}\left(\nabla p_w-\rho_w g\nabla D\right)\right]+c_{hp}R_{pd}+q_w c_{lp}=\frac{\partial}{\partial t}\left(\frac{\phi(1-f_{ip})s_w c_{lp}}{B_w}\right)+\frac{\partial\left[(1-f_{ip})(1-\phi)\rho_r c_{lpa}\right]}{\partial t} \tag{4}$$

in which, ∇ is the Hamilton operator, which represents the gradient of the subsequent quantity; $\vec{k}$ is the absolute permeability tensor in um^2; k_{ro} and k_{rw} are the relative permeabilities of oil and water; μ_o is the viscosity of the oil phase in mPa·s; μ_{we} is the effective viscosity of the water phase in mPa·s; B_o and B_w are the oil and water formation volume factor in m^3/m^3; p_o and p_w are the pressures of the oil and water phase in Pa; ρ_o and ρ_w are the oil and water densities in kg/m^3, and g is the gravitational acceleration in m/s^2. D is the vertical height in m; q_o and q_w are the source/sink terms for oil and water phase in $m^3/(day\cdot m^3)$; ∂ is the symbol used to

denote partial derivatives, and t is the time in day. ϕ is the porosity; s_o and s_w are the oil and water phase saturation. The permeability reduction factor $R_k = 1 + (RRF - 1) \times C_{pa}/C_{pa\max}$, where RRF is the residual resistance factor; c_{pa} and $c_{pa\max}$ are the polymer adsorption concentration and maximum polymer adsorption concentration in kg/m^3. c_{hp} and c_{lp} are the high, and low molecular weight polymer concentrations in kg/m^3; R_{pd} is the polymer degradation rate in day^{-1}, and f_{ip} is the inaccessible pore volume factor. ρ_r is the rock density in kg/m^3, while c_{hpa} and c_{lpa} are the adsorption concentrations of the high and low molecular weight polymer in kg/m^3.

In addition to the mass conservation equations, the auxiliary equations and state equations are as follows. The auxiliary equations include:

$$s_o + s_w = 1 \tag{5}$$

$$p_{cow}(s_w) = p_o - p_w \tag{6}$$

where $p_{cow}(s_w)$ is the capillary pressure in the water-oil system in Pa, which is a function of water phase saturation. The state equations include:

$$k_{ro} = k_{ro}(s_w) \tag{7}$$

$$k_{rw} = k_{rw}(s_w) \tag{8}$$

$$\rho_o = \rho_o(p_o) \tag{9}$$

$$\rho_w = \rho_w(p_w) \tag{10}$$

$$\phi = \phi(p_r) \tag{11}$$

$$\mu_{we} = \mu_{we}(c_{hp}, v_p) \tag{12}$$

where p_r is the reservoir pressure in Pa, V_p is the velocity of polymer solution in m/day. Equation (12) shows that the effective viscosity of the water phase is not the sole function of the high molecular weight polymer component but is also a function of the polymer solution velocity. Therefore, the relationship between the viscosity of polymer solution and shear rate, one of the rheological properties of polymer solution, can be described in the mathematical model.

Meanwhile, it can be seen from the assumptions, mass conservation equations and Equation (12) that the high molecular weight polymer component was only degraded, and the total polymer concentration retained conservation and followed the mass conservation. This model conformed to the theory of polymer chemistry.

To ensure the stability of computation, the full implicit method was applied to solve the mass conservation equations under the boundary and initial conditions. More details about the fully implicit method can be found in [16]. Finally, pressure was obtained along with production, oil and water phase saturation distribution, as well as the high and low molecular weight polymer concentration.

3 Results and discussion

3.1 Rheology of polymer

The relationship between the viscosity of the polymer solution and polymer concentration is indicated in Figure 1 where their relationship curve shows an excellent power law relationship, which can be written as:

$$\mu_{ps} = 0.0001 \times c_p^{1.7782} \tag{13}$$

where μ_{ps} is the viscosity of the polymer solution in mPa·s, and c_p is the polymer concentration in mg/L. The viscosity of the polymer solution increased with an increase in polymer concentration. The main reason is that the formation of a larger hydrodynamic radius after polymer hydration increases the viscosity of polymer solution with a higher polymer concentration [17]. However, the viscosity of the polymer solution with a concentration of 1,500 mg/L decreases with an increase in shear rate, as shown in Figure 2. The main reason for shear thinning of the polymer solution is that the higher shear rate makes the intertwined polymer molecules collapse, which means that the viscosity of the polymer solution will decrease [18].

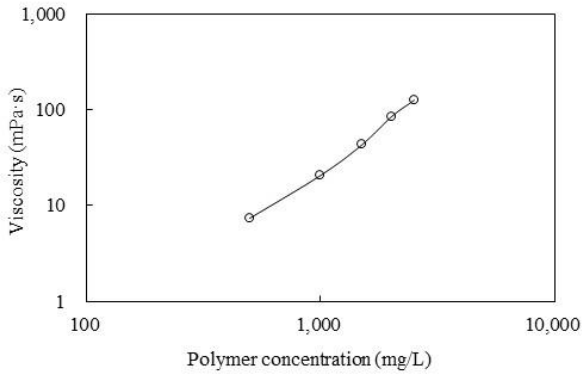

Figure 1. The relationship between the viscosity of the polymer solution and polymer concentration.

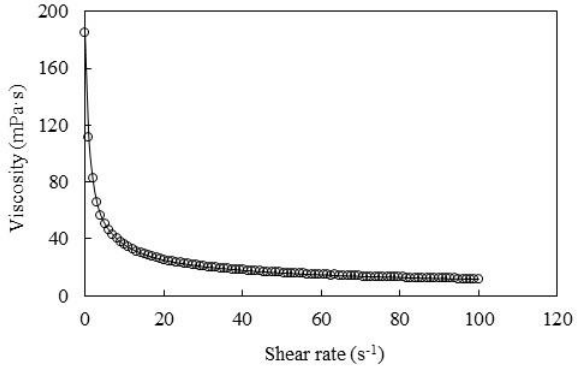

Figure 2. Shear thinning of polymer solution with a concentration of 1,500 mg/L.

3.2 Polymer degradation

Polymer degradation is illustrated in Figure 3. The viscosity of polymer solution decreases with an increase in time. The process of polymer degradation breaks down the long molecular polymer chains; hence, the reduction in length of average molecular chains leads to a decrease in the viscosity of polymer solution [19, 20]. Unlike the

relationship between the viscosity of polymer solution and polymer concentration, the polymer degradation curve shows an excellent exponential relationship, which can be written as:

$$\mu_{ps} = 38.156 \times e^{-0.002 t_{pd}} \quad (14)$$

where t_{pd} is the polymer degradation time in day. Combining the polymer rheological experiment and polymer degradation experiment results, the computational expression of the polymer degradation rate is given:

$$R_{pd} = -\frac{dc_{hp}/c_{hp}}{dt_{pd}} \quad (15)$$

where d is the derivative symbol. Here, the polymer degradation rate can be calculated when its concentration is 1,500 mg/L, which is about 0.001 day^{-1}.

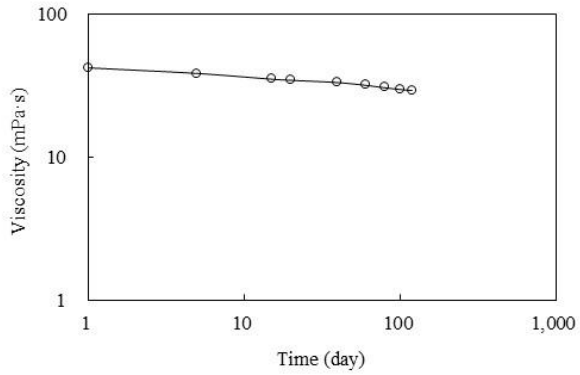

Figure 3. Polymer degradation curve.

3.3 Simulation

3.1.1 Validation

To validate the accuracy of our designed simulator, the simulation results of ECLIPSE V2013.1 software were used to compare with that of our designed simulator because it is a recognized numerical reservoir simulator, and its simulation result is authoritative. Their main input parameters, relative permeabilities, and capillary pressures were the same, which are provided in Table 3 and Table 4. Figure 4 indicates the comparison result of production indicators including pressure differences, oil production, water production, water cut, cumulative oil production, cumulative water production and oil recovery. By comparison, it is clear that the simulation results were very close, the difference between each production indicator was less than 0.2%. The remaining oil saturation distribution after 1,500 days of monitoring by ECLIPSE V2013.1 software and our designed simulator are presented in Figure 5. From the data on the overall remaining oil distribution, the results of both the ECLIPSE V2013.1 software and our designed simulator were very similar. Thus, the accuracy and high reliability of our designed simulator was confirmed.

Table 3. Main input parameters for simulation.

Parameters	Value
Number of blocks along x, m	21
Number of blocks along y, m	21
Number of blocks along z, m	3
Length of the block along x, m	1.4236
Length of the block along y, m	1.4243
Length of the block along z, m	1.3967
Initial porosity, fraction	0.2423
Initial permeability in x-direction, mD	400
Initial permeability in y-direction, mD	400
Initial permeability in z-direction, mD	40
Rock compressibility, MPa^{-1}	2.7×10^{-3}
Rock density, Kg/m^3	2,600
Stock tank oil density, Kg/m^3	880
Initial oil viscosity, mPa·s	8.90
Oil compressibility, MPa^{-1}	1.2×10^{-3}
Oil formation volume factor	1.068
Initial water density, Kg/m^3	1,000
Water viscosity, mPa·s	0.69
Water compressibility, MPa^{-1}	4.26×10^{-4}
Water formation volume factor	1.016
Initial reservoir pressure, MPa	2
initial water saturation, fraction	0.3172
initial oil saturation, fraction	0.6828
Polymer concentration, mg/L	1,500
Polymer degradation rate, day^{-1}	0
Inaccessible pore volume factor, fraction	0.05
Maximum polymer absorption, $K_g/K_{g\ rock}$	1.60×10^{-5}
Residual resistance factor	1.30
Bottom hole pressure of production wells, MPa	2
Injection rate, m^3/day	0.65

Table 4. Relative permeabilities and capillary pressures for simulations.

Sw	Krw	Krow	Pcow
0.3061	0.0000	1.0000	75349
0.3372	0.0001	0.8762	72491
0.3563	0.0017	0.8014	67368
0.3834	0.0031	0.7020	64853
0.4145	0.0055	0.5864	61115
0.4416	0.0099	0.4884	59305
0.4727	0.0150	0.3837	56567
0.5013	0.0231	0.2966	53832
0.5289	0.0381	0.2231	52450
0.5580	0.0612	0.1551	50505
0.5881	0.0912	0.0952	48877
0.6162	0.1293	0.0599	47696
0.6473	0.1810	0.0299	45611
0.6744	0.2272	0.0122	44483
0.7052	0.2884	0.0000	43850

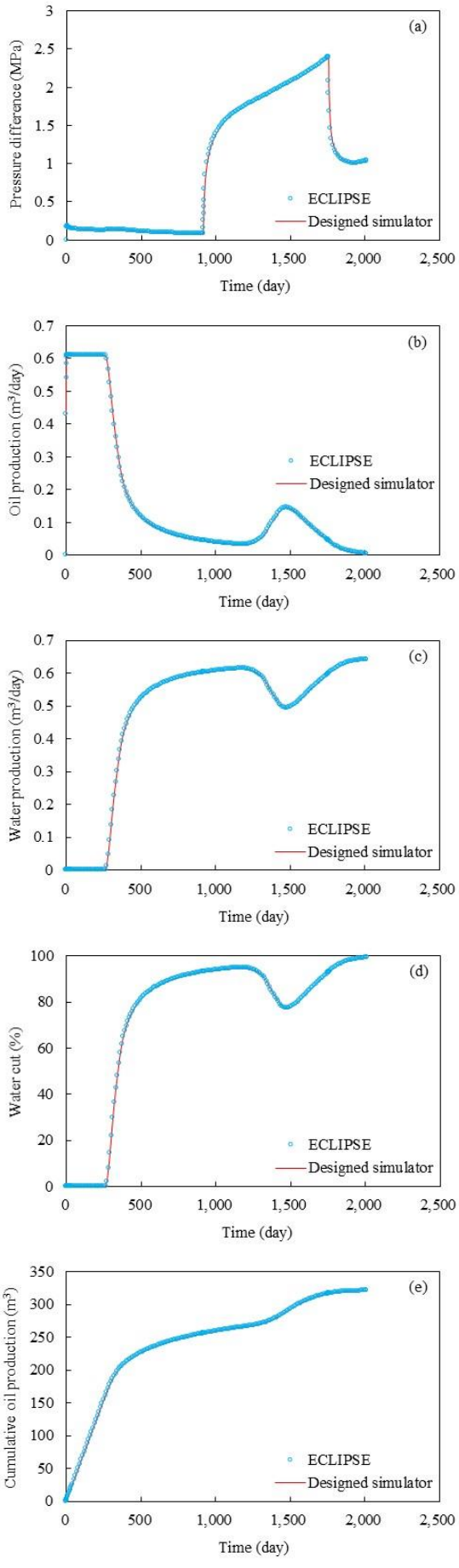

Figure 4. Comparison results of (a) pressure difference, (b) oil production, (c) water production, (d) water cut, (e) cumulative oil production, (f) cumulative water production, and (g) oil recovery of ECLIPSE V2013.1 software and designed simulator.

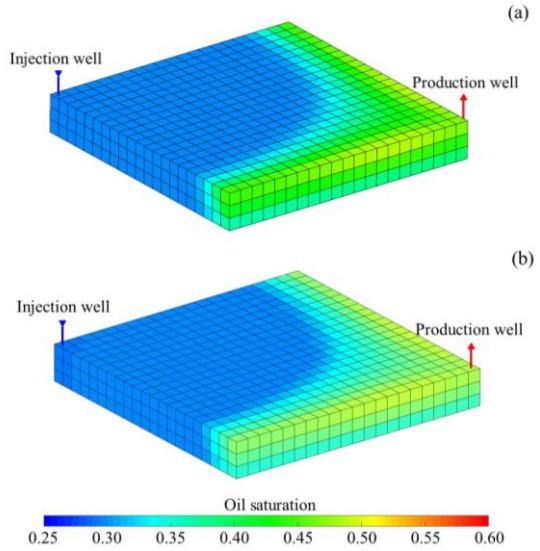

Figure 5. Comparison results of remaining oil saturation distribution after 1,500 days of (a) ECLIPSE V2013.1 software and (b) the designed simulator.

3.1.2 Effect of polymer degradation

Four more simulations were undertaken to analyze the effect of polymer degradation on production indicators. They considered the polymer degradation rate of 0.001 day^{-1}, 0.002 day^{-1}, 0.010 day^{-1} and 0.100 day^{-1}. The rest of the parameters were the same. Figure 6 provides the comparison result of production indicators at different polymer degradation rates. This figure demonstrates that the higher polymer degradation rate could cause a more

significant impact on production indicators. The reduction of production indicators caused by polymer degradation after 1,500 days is shown in Table 5. Figure 7 shows the remaining oil saturation distribution after 1,500 days of simulation considering the polymer degradation rate of 0.100 day^{-1}. From this figure, the remaining oil saturation of the simulation considering the polymer degradation rate of 0.100 day^{-1} was more than that of the simulation considering the polymer degradation rate of 0 day^{-1}, as seen in the comparison between Figure 5 and Figure 7. Notably, the oil recovery, one of the most critical production indicators, decreased 6% after 2,000 days.

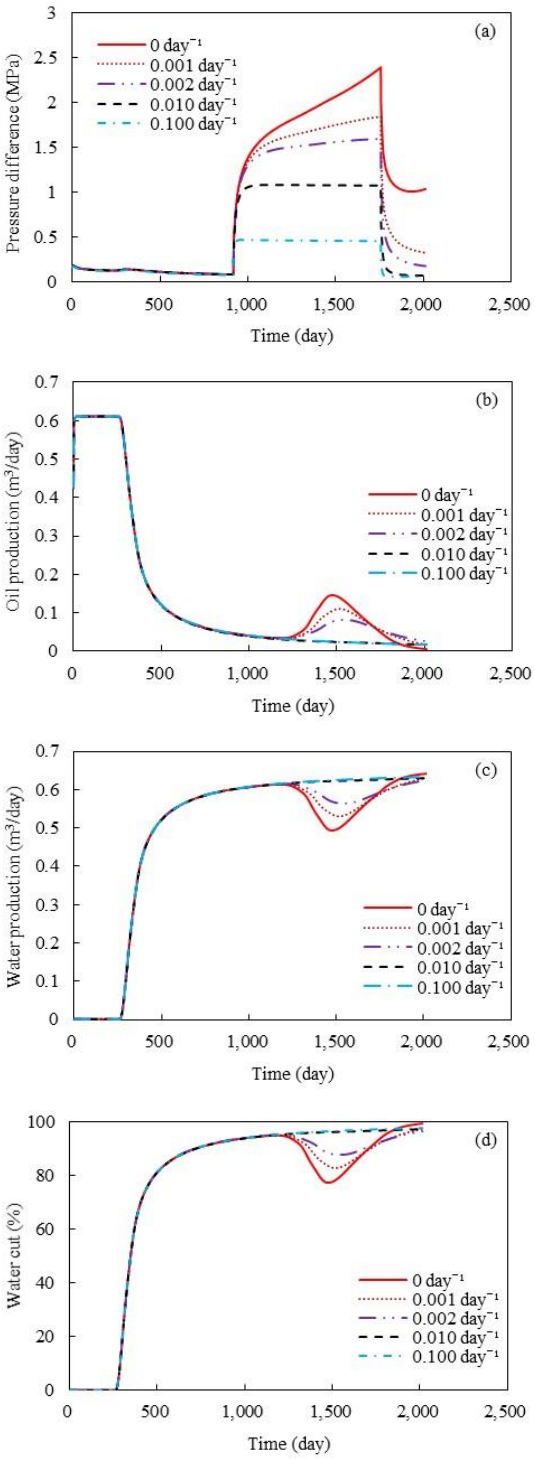

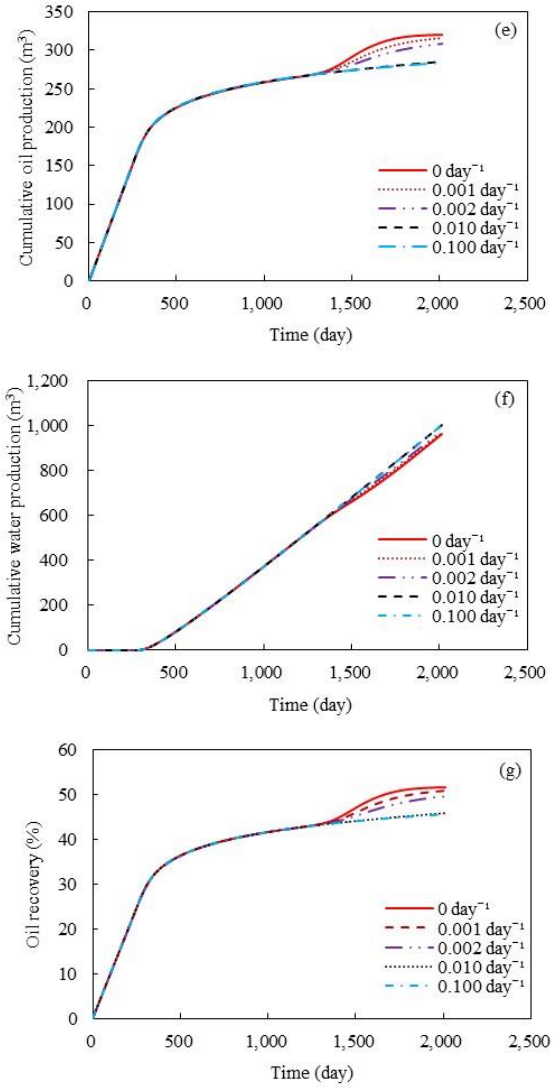

Figure 6. Comparison results of production indicators including (a) pressure difference, (b) oil production, (c) water production, (d) water cut, (e) cumulative oil production, (f) cumulative water production, and (g) oil recovery at different polymer degradation rates.

Table 5. Reduction of production indicators caused by polymer degradation after 1,500 days.

Production indicators	Polymer degradation rate, day^{-1}			
	0.001	**0.002**	**0.010**	**0.100**
Pressure difference, MPa	0.32	0.51	0.99	1.61
Oil production, m^3/day	0.03	0.06	0.12	0.12
Water production, m^3/day	-0.03	-0.07	-0.13	-0.13
Water cut, %	-5.07	-10.04	-18.46	-18.78
Cumulative water production, m^3	6.55	11.09	18.25	18.55
Cumulative oil production, m^3	-7.24	-12.22	-20.05	-20.41
Oil recovery, %	1.06	1.79	2.94	2.99

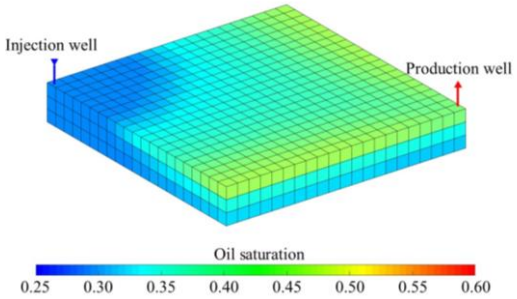

Figure 7. Remaining oil saturation distribution after 1,500 days of the simulation considering the polymer degradation rate of 0.100 day^{-1}.

4 Conclusions

The primary objective of this paper was to investigate the effect of polymer degradation on polymer flooding in a homogeneous reservoir to provide a theoretical guide for the development of similar oilfield reservoirs. The results of the physical experiment indicate that the relationship between the viscosity of the polymer solution and polymer concentration had a good power law relationship; the viscosity of the polymer solution increased with the increase of the polymer concentration. However, it decreased with an increase in shear rate; the rheological property of polymer solution indicated shear thinning performance. Moreover, the polymer degradation led to a viscosity reduction of polymer solution with the increase of time, and there was an excellent exponential relationship. Based on the physical experiment and mathematical model proposed in this paper, the polymer degradation rate was introduced and calculated. Furthermore, the 3D two-phase polymer flooding simulator that considered the polymer degradation was designed and validated with high accuracy and reliability when compared to the simulation results run in ECLIPSE V2013.1 software. The results of the simulation considering the polymer degradation indicates that the polymer degradation significantly influenced the production indicators. In the simulation considering the polymer degradation rate of 0.100 day^{-1}, the recovery factor after 2,000 days was 6% lower than that in the simulation without considering the polymer degradation. To minimize the impact of the polymer degradation on polymer flooding, some methods have been proposed [4, 21], which should be followed by a reduction in polymer degradation to increase polymer flooding efficiency.

This work was supported by the National Science and Technology Major Project of China (No.2016ZX05025-001-005)

References

1. Q. Wei, X. Zhang, H. Wang, Curr. Opin. Colloid. Interface. Sci., **35**, 36-41 (2018)
2. X. Zhang, Y. Chen, J. Hu, Pro. Aerosp. Sci., 97, 22-34 (2018)
3. R. Liu, W. Pu, D. Du, J. Gu, L. Sun, J Petro. Sci. Eng, **164**, 467-484 (2018)
4. D.C. Standnes, I. Skjevrak, J Petro. Sci. Eng, **122**, 761-775 (2014)
5. X. Xin, Y. Li, G. Yu, W. Wang, Z. Zhang, M. Zhang, W. Ke, D. Kong, K. Wu, Z. Chen, Energies, **10** (2017), doi:10.3390/en10111698
6. A.A. Alquraishi, F.D. Alsewailem, Carbohydr. Polym., **88**, 859-863 (2012)
7. M. Algharaib, A. Alajmi, R. Gharbi, J Petro. Sci. Eng, **115**, 17-23 (2014)
8. J. Choi, D. Ka, T. Chung, J. Jung, G. Koo, T. Uhm, S.H. Jung, S. Park, H.T. Jung, Macromolecular Research, **23**, 518-524 (2015)
9. S. Cai, X. He, K. Liu, R. Zhang, L. Chen, Iran. Polym. J, **24**, 663-670 (2015)
10. Y. Ma, J. Hou, Oilfield Chemistry, **34**, 361-365 (2017)
11. A. Li, H. Song, H. Xie, Petroleum Geology and Recovery Efficiency, **23**, 70-74 (2016)
12. G. Zhao, J. Fang, B. Gao, Y. Wang, A. Chen, D. Wang, C. Dai, Oilfield Chemistry, **32**, 62-66 (2015)
13. J. Wang, H. Liu, J. Ind. Eng. Chem, **20**, 656-667 (2014)
14. E. Unsal, A. Berge, D.A.Z. Wever, J Petro. Sci. Eng, **163**, 671-682(2017)
15. B.I. Choi, M.S. Jeong, K.S. Lee, Polym. Degrad. Stab, **110**, 225-231 (2014)
16. Z. Chen, G. Huan, Y. Ma, *Computational Methods for Multiphase Flows in Porous Media* (Society for Industrial and Applied Mathematics, Philadelphia, USA, 2006)
17. D. Fang, R. Guo, H. Hua, *Acrylamide polymer* (Chemical Industry Press, Beijing, 2006)
18. G. Lu, N. Shao, M. Cao, B. Wang, Engineering Plastics Application, **44**, 90-92 (2016)
19. A.M. Mansour, R.S Al-Maamari, A.S Al-Hashmi, A. Zaitoun, H. Al-Sharjic, J Petro. Sci. Eng, **115**, 57-65 (2014)
20. L.F.L. Oliveira, D.J. Schiozer, M. Delshad, J Petro. Sci. Eng, **147**, 346-355 (2016)
21. L.J. Giraldo, M.A. Giraldo, S. Llanos, G. Maya, R.D. Zabala, N.N. Nassar, C.A. Franco,V. Alvarado, F.B. Cortés, J Petro. Sci. Eng, **159**, 841-852 (2017)